# Multi-physics Performance Assessment for High Temperature Disposal Concept of Spent Nuclear Fuel

Samuel Park[a], Nakkyu Chae[b], Seungjin Seo[c], Sungyeol Choi[a, d, e]
[a]*Department of Nuclear Engineering, Seoul National University, Gwanak-gu, Seoul, Republic of Korea*
[b]*Disposal Performance Demonstration Research Division, Korea Atomic Energy Research Institute, Daejeon, Republic of Korea*
[c]*Disposal Performance Demonstration Research Division, Korea Atomic Energy Research Institute, Daejeon, Republic of Korea*
[d]*Nuclear Research Institute for Future Technology and Policy, Seoul National University, Gwanak-gu, Seoul, Republic of Korea*
[e]*Institute of Engineering Research, Seoul National University, Gwanak-gu, Seoul, Republic of Korea*

[*]Corresponding author: choisys7@snu.ac.kr

***Keywords: High Temperature Disposal Concept, HADES, Two-phase flow, Richards' flow,***

## 1. Introduction

With the increasing amount of Spent Nuclear Fuel (SNF), many countries operating Nuclear Power Plants (NPPs) have sought solutions for SNF storage and disposal. One promising solution is the KBS-3 type disposal concept, developed by Finland and Sweden. The concept consists of an Engineered Barrier System (EBS) and a Natural Barrier System (NBS) [1]. The EBS includes a copper canister, with withstands mechanical and chemical loads, and a bentonite buffer, which retards groundwater inflow and radionuclide release. The NBS is the host rock, which prevents radionuclide migration. The primary concept of the design is based on a thermal criterion of 100℃, aimed at preventing unexpected incidents such as phase change in the bentonite buffer that could degrade its material properties.

Despite this thermal limitation, there have been focused efforts to elevate the maximum temperature up to 150℃ and 200℃ by embedding more SNF into a canister or reducing the distance between boreholes [2]. Similarly, in Korea, there are numerous efforts to assess the performance of a Deep Geological Repository (DGR) under a high temperature disposal concept. However, these efforts have not accurately estimated Thermal-Hydraulic (TH) behaviors, because they have focused solely on thermal behavior [3].

To address this problem, HADES (High-level rAdiowaste Disposal Evaluation Simulator) was developed to assess the fully-coupled TH performance for high temperature disposal concepts [4]. The code was validated by comparing experimental results conducted under high temperature conditions and was applied to a high-temperature disposal design by reducing the distance between boreholes in the Korean Reference disposal System (KRS). Additionally, the limitations of the approximated Richards' approach, commonly used in general two-phase flow simulations, were highlighted by comparing it to a more general two-phase approach.

## 2. Methodology

In the DGR environment, various thermal, hydraulic, mechanical, chemical, and electrochemical behaviors occur. These behaviors are interconnected, influencing one another, as shown in Fig. 1. Therefore, in order to accurately estimate the multi-physics behavior within the DGR, it is crucial to consider these various mutual relations.

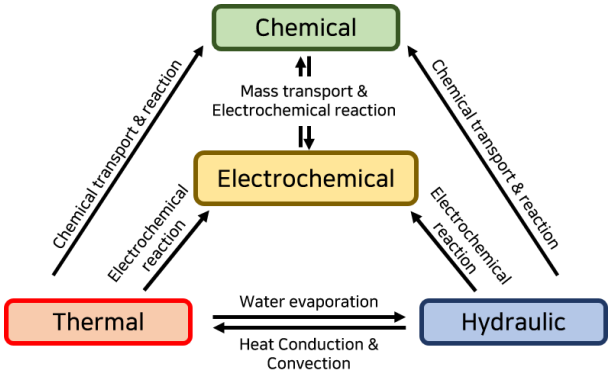


Fig. 1. Mutual relations among THC-EC behaviors in the DGR environment as considered in HADES.

### *2.1 Code Structure*

HADES was developed for estimating the multi-physics behavior of a DGR using FEM (Finite Element Method) based open-source numerical code. It is based on the MOOSE (Multiphysics Object Oriented Simulation Environment) framework [4]. Although HADES includes own mesh generation and data analysis applications, two additional open-source software tools, Gmsh (a finite element mesh generation software) and Paraview (a data analysis tool), are utilized to study the multi-physics behavior of DGR, as illustrated in Fig. 2.

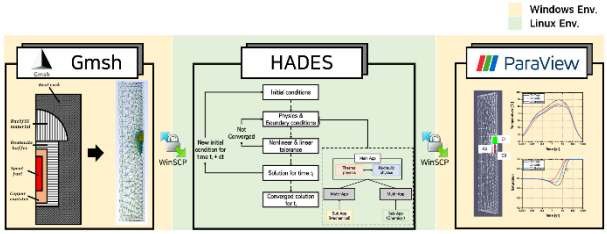


Fig. 2. Code structure and algorithm of HADES

*2.2 Governing Equations*

HADES can solve the mutual relations between THC-EC behaviors; however, the focus here is on thermal and hydraulic behavior. To model TH behavior under DGR conditions, HADES employs two approaches: the general two-phase and the Richards' (approximation of general two-phase) approaches. The primary difference between these methods lies in the treatment of the gas phase. In the Richards' approach, the dry air pressure is assumed to be constant, whereas the general approach calculates the dynamic behavior of the gas phase, as exhibited in Fig. 3.

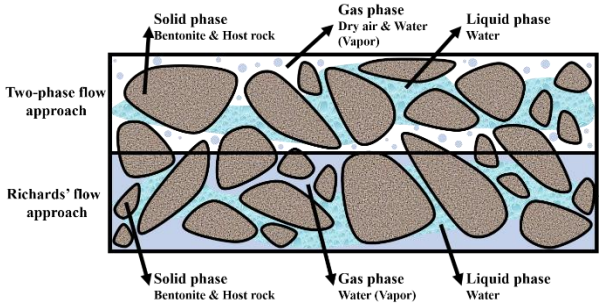


Fig. 3. Three phase consideration of general and approximated approaches of porous media.

Equations (1) to (5) describe the hydraulic governing equations for porous media. Equations (1) and (2) represent the governing equation for the general two-phase and Richards' approaches, respectively. Equations (3) to (5) detail the water advection, vapor advection, and vapor diffusion, respectively.

$$\frac{\partial}{\partial t}\left(\phi\left(S^l\rho_w^l + S^g\rho_w^g\right)\right) + \nabla \cdot \left(J_w^{A,l} + J_w^{A,g} + J_w^{D,g}\right) = Q \quad (1)$$

$$\frac{\partial}{\partial t}\left(\phi\left(S^l\rho_w^l + S^g\rho_w^g\right)\right) + \nabla \cdot \left(J_w^{A,l} + J_w^{D,g}\right) = Q \quad (2)$$

$$J_w^{A,l} = -\rho^l \frac{\boldsymbol{k}k_{rel}^l}{\mu^l}(\nabla P^l - \rho^l g) \quad (3)$$

$$J_w^{A,g} = -\rho^g \frac{\boldsymbol{k}k_{rel}^g}{\mu^g}(\nabla P^g - \rho^g g) \quad (4)$$

$$J_w^{D,g} = -\rho^g D_w^g \nabla\left(\frac{\rho_w^g}{\rho^g}\right) \quad (5)$$

where $\phi$ is the porosity of the porous media, $S^l$ is the degree of saturation of liquid phase, $S^g$ is the degree of saturation of gaseous phase calculated as $1 - S^l$, $J_w^{A,l}$ is the advective flux of water component in liquid phase [kg/(m2·s)], $J_w^{D,g}$ is the diffusive flux of the water vapor component in gas phase [kg/(m2·s)], Q is the source/sink term [kg/(m3·s)], **k** is the intrinsic permeability of the porous medium [m2], $k_{rel}^l$ is the relative permeability of liquid phase, $\mu^l$ is the dynamic viscosity of liquid phase [Pa·s], g is gravitational acceleration [m/s2], and $D_w^g$ is the effective diffusion coefficient considering of tortuosity of water component in the gas phase [m2/s].

Equation (6) to (10) describe the thermal governing equations for porous media. Equation (6) and (7) present the governing equations for thermal behavior under the general two-phase and Richards' flow approaches, respectively. Equation (8) to (10) explain heat transfer mechanisms through water advection, vapor advection, and thermal conduction, respectively.

$$\frac{\partial}{\partial t}\Big((1-\phi)\rho^s C_p^s T + \phi S^l \rho^l C_p^l T + \phi S^g \rho^g C_p^g T\Big) + \nabla \cdot \left(J_w^{A,l} + J_w^{A,g} + J_w^{D,g}\right) = Q \quad (1)$$

$$\frac{\partial}{\partial t}\left(\phi\left(S^l\rho_w^l + S^g\rho_w^g\right)\right) + \nabla \cdot \left(J_w^{A,l} + J_w^{D,g}\right) = Q \quad (2)$$

$$J_w^{A,l} = -\rho^l \frac{\boldsymbol{k}k_{rel}^l}{\mu^l}(\nabla P^l - \rho^l g) \quad (3)$$

$$J_w^{A,g} = -\rho^g \frac{\boldsymbol{k}k_{rel}^g}{\mu^g}(\nabla P^g - \rho^g g) \quad (4)$$

$$J_w^{D,g} = -\rho^g D_w^g \nabla\left(\frac{\rho_w^g}{\rho^g}\right) \quad (5)$$

where $\rho^s$ is the density of porous media [kg/m$^3$], $C_p^s$ is the specific heat of solid phase [J/(kg·K]], and $\lambda_{eff}$ is the effective thermal conductivity [W/(mK)].

*2.3 Input parameters*

Due to the asymmetrical arrangement, a quarter of the canister are utilized as the geometry to estimate TH behavior. Since the distances between the borehole and disposal tunnel are 7.5m and 40m, respectively, the analysis region is 3.75m and 20m, respectively. Additionally, to analyze TH behavior under a high-temperature disposal concept, various reduced borehole distances of 7m, 6m, 5m, and 4m are considered. The diameters of canister and bentonite are 1.03m and 2.02m, respectively, while their height are 4.78m and 7.78m, respectively, as shown in Fig. 4 [5].

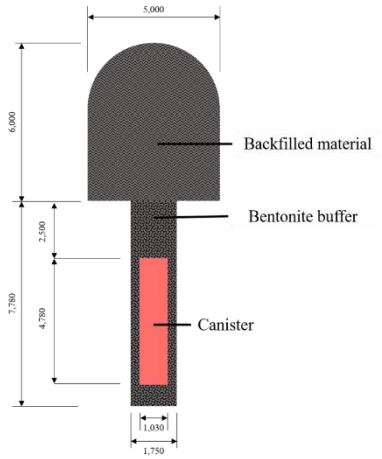


Fig. 4. Schematic design of single borehole of KRS

As an EBS, KJ-II bentonite and 30:70 bentonite-sand mixture backfilled material, and NBS, crystalline hostrock were utilized. The thermal and hydraulic material properties are summarized in Table 1 [4].

Table 1. Thermal and hydraulic material properties of KRS

| Parameter | Symbol | Bentonite | Backfilled material | Host rock |
|---|---|---|---|---|
| Dry Density [kg/m$^3$] | $\rho$ | 1600[a] | 1600* | 2650* |
| Porosity | $\phi$ | 0.41[b] | 0.4* | 0.0116[d] |
| Thermal conductivity (Dry) [W/(mK)] | $\lambda_{dry}$ | 0.6611[a] | 1.00* | 3.05[d] |
| Thermal conductivity (Wet) [W/(mK)] | $\lambda_{wet}$ | 1.2243[a] | 2.00* | 3.31[d] |
| Specific heat (Dry) [J/(kg K)] | $C_{p,dry}$ | 894[c] | 980* | 820[d] |
| Specific heat (Wet) [J/(kg K)] | $C_{p,wet}$ | 1337[c] | 980* | 820[d] |
| Intrinsic permeability of liquid [m$^2$] | $K$ | 2.56E-20[b] | 1.6E-19* | 1.0E-18[e] |
| Relative permeability of liquid | $K_{Rel}$ | $S_l^{3.0*}$ | $S_l^{1.9*}$ | $S_l^{3*}$ |
| Van Genuchten (alpha) [Pa$^{-1}$] | $\alpha$ | 2.6E-7[d] | 3.3E-7* | 5E-7* |
| Van Genuchten (lambda) | $\lambda$ | 0.2941[d] | 0.5* | 0.6* |
| Residual saturation | $S_r$ | 0.01* | 0.01* | 0.01* |

a Yoon et al: https://doi.org/10.3390/en11092269
b Yoon et al: https://doi.org/10.1016/j.heliyon.2023.e18447
c Yoon et al: https://doi.org/10.7733/jnfcwt.2017.15.3.199
d Lee et al: https://doi.org/10.1016/j.tust.2020.103452
e Ko et al: https://doi.org/10.7733/jnfcwt.2019.17.S.15
*: Assumed value

The initial and boundary conditions utilized in the analysis are summarized in Fig. 5. The initial temperature and degree of saturation of bentonite are 25℃ and 0.6, respectively, while the hostrock has a temperature gradient of 30 ℃/km and a degree of saturation of 1, considering the hydrostatic gradient. The decay heat from canister follows equation (11). The boundary conditions of top and bottom of the hostrock maintain a constant temperature and constant hydrostatic pressure, while the side surface of the bentonite is set to impermeable and adiabatic conditions.

$$2.683 \times 10^4 \times (t + 40)^{-0.758} \quad (11)$$

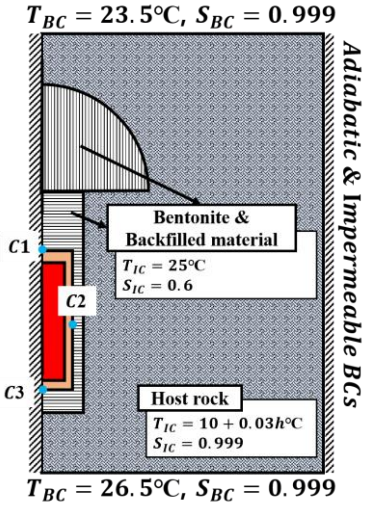


Fig. 5. Schematic design of initial and boundary conditions of DGR environment

## 3. Results and Discussions

### *3.1 Benchmark (CTF1 Exp.)*

In order to validate the TH behavior under high temperature condition, the CTF1 Exp., conducted by CIEMAT, is utilized as a benchmark case [6]. In this experiment, the thermal boundary conditions include a heater set to 120℃ on the left-hand side and adiabatic boundary condition on the right-hand side. In addition, the setup maintains impermeable conditions at the side surface, as illustrated in Fig. 6.

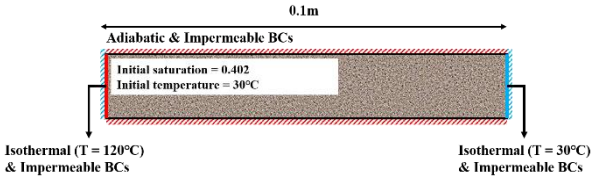


Fig. 6. Schematic design of the initial and boundary conditions in the CTF1 Exp.

Fig. 7 shows the degree of saturation results of high and low permeability porous media conditions. According to the results, both the Richards' and two-phase flow approaches accurately estimate the experimental results under high permeability conditions. However, under low permeability conditions, only the two-phase flow approach provide an accurate estimation of the experimental results.

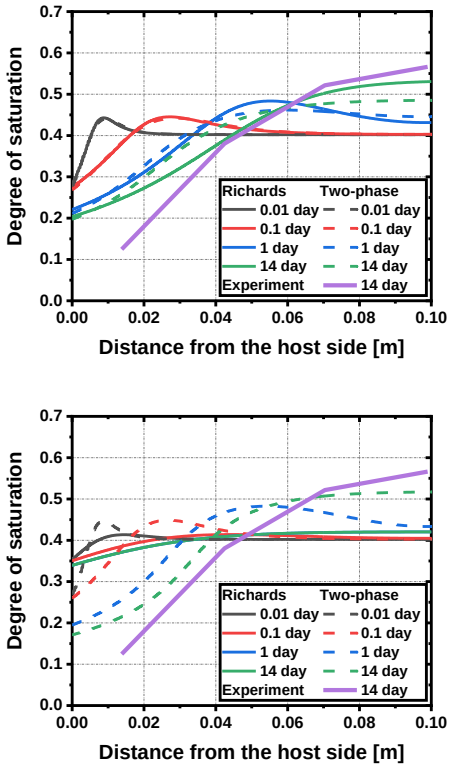


Fig. 7. Evolutions and distributions of the degree of saturation evaluated by the Richards approach (solid line), the general two-phase flow (dash line) approaches, and experimental results (purple thick solid line). The top results considered high permeability porous media, while the bottom results considered low permeability porous media.

Fig. 8 illustrates the reason for the difference between the Richards' and two-phase flow approaches by showing gas pressure behavior. According to the Fig. 7, although both low and high permeability conditions exhibit similar gas pressure accumulation in the left heating region, the magnitude of pressure accumulation is higher under of low permeability condition. It indicates that the more gas accumulates in low permeability condition.

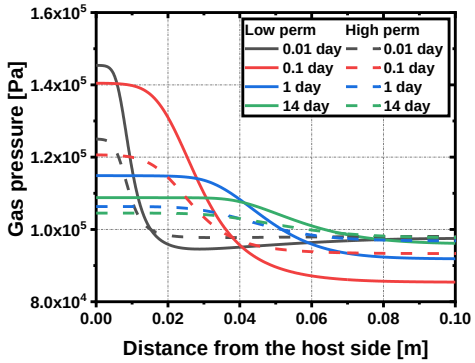


Fig. 8. Gas pressure evolutions and distributions of low (solid line) and high (dash line) permeability conditions

*3.2 TH behavior estimations*

Figure 9 shows the evolution of peak temperature and minimum degree of saturation with varying borehole distances, ranging from 8m to 5m. According to the results, the maximum temperatures and minimum saturations evolutions calculated by two-phase and Richards' approaches are nearly identical, even under different borehole distance conditions. When the borehole distances are 8m, 7m, 6m, and 5m, the peak temperatures are 112.8℃, 104.6℃, 97.9℃, and 95.5℃, respectively. However, the effect of borehole distance on saturation evolution is not significant.

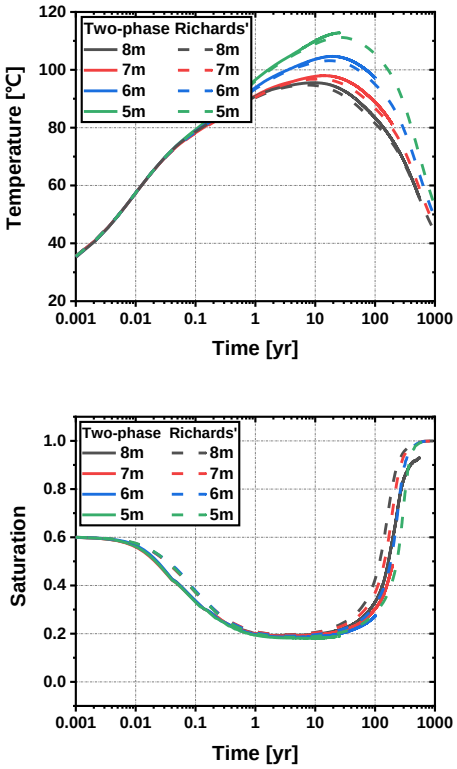


Fig. 9. Evolutions of peak temperature (upper figure) and minimum degree of saturation of canister-bentonite interface, calculated using the two-phase flow (solid line) and Richards' (dash line) approaches.

*3.3 Applicability of Richards' flow to high temperature DGR condition*

The Richards' flow approach, an approximation of the general two-phase flow, offers significant advantages due to its inherent simplicity. By assuming constant gas pressure, it avoids the need to account for gas pressure changes, which simplifies the calculations. However, this approach has significant limitations, particularly in environments where significant pressure accumulation occurs, such as in low permeability and high temperature conditions, as shown in Fig. 7. In these scenarios, the Richards' approach may not provide accurate results.

However, the difference between the two approaches is not critical under high temperature DGR conditions. The estimated results for temperature and degree of saturation are almost identical, with only slight differences. Therefore, regardless of the DGR condition, including scenarios with current peak temperature of 100℃, both the Richards' and two-phase approaches can be applied to high temperature DGR conditions exceeding 100℃.

## 4. Conclusions

In this study, TH behavior under high temperature DGR is estimated using the HADES numerical code. In order to validate the HADES code for high temperature DGR condition, the CTF1 Exp. is utilized, and the estimated TH behaviors are found to closely match the experimental results. For high temperature DGR conditions, with borehole distances of 5m, 6m, 7m, and 8m, the peak temperature at the canister-bentonite interface are 95.5℃, 97.9℃, 104.6℃, and 112.8℃, respectively. Additionally, the applicability of the Richards' flow approach is examined. While the Richards' flow approach, an approximated approach of general two-phase flow approach, has significant limitation, particularly in conditions with dramatic pressure change. However, the Richards' flow approach can still be applied to high temperature DGR conditions and provides results comparable to those of the general two-phase flow approach.

## REFERENCES

[1] S. Petterson, and B. Lonnerberg, Final Repository for Spent Nuclear Fuel in Granite – The KBS-3V Concept in Sweden and Finland, *16 – 18 Jun 2008*
[2] F. Kober, R. Schneeberger, S. Vomvoris, S. Finsterle, and B. Lanyon, The HotBENT Experiment: Objectives, Design, Emplacement and Early Transient Evolution, *18 Oct, 2023.*
[3] J. Y. Lee, K. I. Kim, I. Y. Kim, H. J. Ju, J. T. J, C. S. Lee, J. W. Kim, and D. K. C, High-efficiency Deep Geological Repository System for Spent Nuclear Fuel in Korea with Optimized Decay Heat in a Disposal Canister and Increased Thermal Limit of Bentonite, *vol 55, 2023.*
[4] S. Park, N. K. Chae, P. H. Ju, S. J. Seo, R. I. Foster, S. Y. Choi, Coupled 3D Thermal-Hydraulic Code Development for Performance Assessment of Spent Nuclear Fuel Disposal System, *in press.*
[5] J. Y. Lee, H. A. Kim, I. Y. Kim, H. J. Choi, D. K. Cho, Analyses on Thermal Stability and Structural Integrity of the Improved Disposal System for Spent Nuclear Fuels in Korea, *vol. 18, pp. 21-36, 2020.*
[6] W. Wang, J. Rutqvist, U. J. Gorke, J. T. Birkholzer, O. Kolditz, Non-isothermal Flow in Low Permeable Porous Media: a Comparison of Richards' and Two-phase Flow Approaches, *vol 62, pp. 1197-1207, 2011.*